Synthesis and Characterization of $CoMo/Al_2O_3$-MgO-(X) catalysts doped with alkaline oxides (K, Li)

D. Solis*
Facultad de Química, UAEM
Paseo Tollocan y Paseo Colón s/n Toluca, 50000, México;

J. Ramírez♣, R. Cuevas, R. Contreras
UNICAT, Departamento de Ingeniería Química
Facultad de Química, UNAM

T. Cortéz
♣*Instituto Mexicano del Petróleo*
Eje Central Lázaro Cárdenas 152, México D.F. 07730. México

M. Aguilar
Instituto de Física, UNAM
(Recibido: 17 de marzo de 2006; Aceptado: 25 de septiembre de 2007)

CoMo catalysts were prepared using Al_2O_3-MgO-(X) hybrid supports, where X = K_2O or Li_2O. The textural, structural and acid-base properties of these materials were characterized by several techniques. The catalysts were preliminarily evaluated in the hydrodesulfurization (HDS), hydrogenation (HYD) and hydrocracking (HCK) model reactions. The aims of this work are to identify the effect of the addition of an alkaline oxide (either K_2O or Li_2O) to the Lewis acid sites in the $CoMo/Al_2O_3$-MgO formulation; and on the other hand, to establish a relationship between the acidity and the catalytic performance (hydrogenation function). The results obtained from the pyridine thermodesorption analysis and the n-butyl amine titration techniques show that the incorporation of an alkaline oxide to the $CoMo/Al_2O_3$-MgO formulation causes a slight decrease in the total number of acid sites (TNAS) with respect to Al_2O_3 and the Al_2O_3-MgO hybrid supports. Both the enhanced textural and structural stability of the $CoMo/Al_2O_3$-MgO-(X) catalytic formulations, which could be probably attributed to the incorporation of Li or K cations to the MgO framework, stabilizing it, can also be observed. As for the catalytic performance, the $CoMo/Al_2O_3$-MgO-(X) catalysts containing either Li_2O or K_2O, show a decrease in both the HYD and HYC conversions; however, the formulation containing Li_2O shows the best catalytic behavior due to both the low n-octane yield and the low hydrocracking activity.

Keywords: Lithium; Potassium; Magnesia; Acid sites; Hydrodesulfurization; Hydrogenation

1. Introduction

In order to fulfill the restrictions on sulfur content in transport fuels, it is necessary to adequate both the hydrotreating (HDT) catalysts and processes. Although the sulfur compounds present in fuels are not difficult to eliminate, it has been reported that during the hydrotreatment of the FCC (fluid catalytic cracking) naphtha in some industrial facilities, the hydrogenation of unsaturated compounds occurs at some extent, promoting the undesirable decrease in the octane number which measures the explosive power in gasoline [1-2].

The aforementioned means that during the HDT, under the standard operation conditions of the hydrodesulfurization (HDS) of the FCC naphtha, the olefinic compounds (which represent 20-60 % v/v) undergo saturation. Consequently, the octane number decreases up to 10 units; and this has important consequences because the fuel quality decreases. Therefore, it is necessary to control the hydrodesulfurization, hydrogenation and hydrocracking functions. In order to obtain a good balance between the catalytic functionalities stated above, the use of the precursor of the active CoMo phases instead of NiMo in the catalysts, at low operation pressures, is proposed. Although CoMo catalysts present a low hydrogenation activity, it is powerful enough to hydrogenate unsaturated compounds; and the operation at low pressure leads to catalyst deactivation due to coke deposition.

To take advantage of these problems, some researchers have reported that the use of a catalytic support with less acidity inhibits the hydrogenation activity; this alternative could be also promoted by the addition of a low acidity material to the commercial Al_2O_3 support; these low-acidity materials could be CaO, ZnO or MgO [3-7]. Amongst the mentioned supports, the most studied is the MgO, which was firstly reported by Zdrazil [3] and Klimova [4], and recently by other researchers [5-8].

*solis_casados@yahoo.com.mx

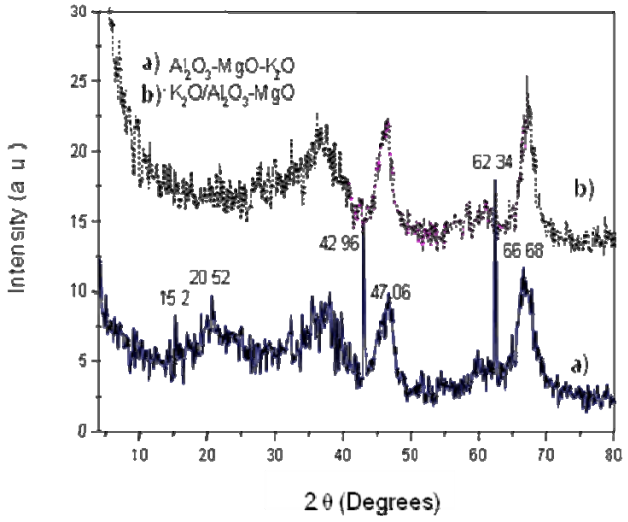

Table 1. Textural properties of the synthesized supports: specific area (S_{BET}), pore volume (V_P) and mean pore diameter (D_P).

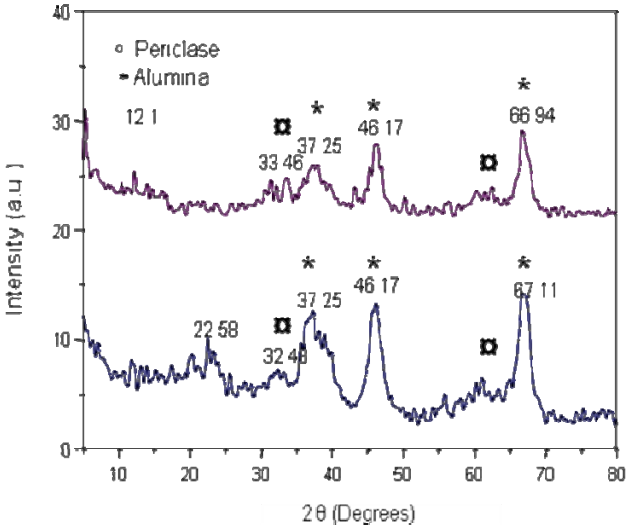

Table 2. Textural properties of the prepared catalysts: specific area (S_{BET}), pore volume (V_P) and mean pore diameter (D_P).

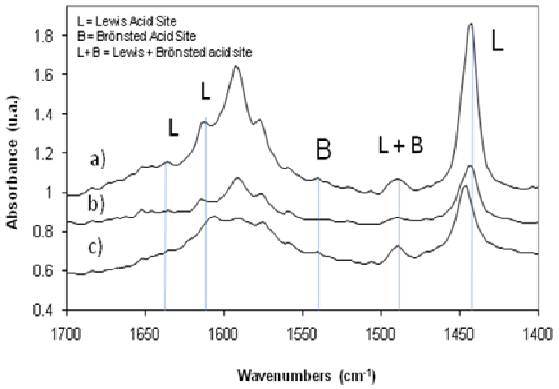

Figure 3. FT-IR Spectra of the pyridine thermodesorption of: a) Al_2O_3, b) Al_2O_3-MgO; and c) Al_2O_3-MgO-K_2O.

Some disadvantages of the magnesia support are the low specific surface area, low textural stability in the presence of water and the formation of $Mg(OH)_2$ and $Mg(CO_3)_2$ on the support surface when exposed to room conditions [3,8]. By taking into account the aforesaid, it is advisable that not only the catalysts be supported on magnesia, but also that hybrid supports containing magnesia be prepared by non-aqueous impregnations [3-9], which increases the cost of the catalyst. In addition, on pure magnesia supports, it has been supposed the existence of undesirable interactions with the active phase precursors (Mo and Co) during impregnation [3-4] when aqueous solutions are used. It has been supposed that metals with ionic radii similar to that of Mg, promote the formation of the substitutional solid solution; in this case, it has been proposed that in the MgO framework, the Mg atoms are substituted by Co atoms, which have closer ionic radii [10].

T. Klimova et al. [4] reported that the addition of MgO to the $NiMo/Al_2O_3$ formulation, in molar ratios of $[MgO/Al_2O_3+MgO]$ = 0.0, 0.05, 0.25, 0.50, 0.75 and 1.0, changes the catalytic performance, decreasing the HYD activity, which was followed through the HDS of the thiophene molecule, specifically through the butane production. In this work, the possibility of the formation of a NiO-MgO solid solution was reported. Afterwards, Mohan-Rana et al. [5] found that the introduction of MgO to alumina modifies the metal-support interaction of the active metals, which provides a better hydrogenolysis function. The latter could be explained as follows: as the mixture of MgO and the Al_2O_3 supports occurs, it modifies the interaction behavior towards the MoS_2 phases; and consequently the HDS activity increases.

According to the results reported above, the decrease in the acid properties of the support as a result of the MgO addition is expected; and it is correlated with the decrease found in the hydrogenation (HYD) and hydrocracking (HCK) activity.

According to these facts, the Al_2O_3-MgO system obtained from conventional preparations is an alternative to be taken into account. In addition, when CoO is deposited on the Al_2O_3–MgO supports, it has been concluded [11] that with a small MgO content in the formulation, the cobalt oxide has a better dispersion. The use of high quantities of magnesia apparently promotes the Mg-Co interaction, yielding the $Co_xMg_{1-x}O$ solid solution in the crystalline framework.

Additionally, for both alumina and magnesia supports, it has been proved [12-13] that with the addition of an alkaline compound to the catalytic formulation, such as K and Li; and also lanthanides such as La, promotes not only a decrease in the number of acid sites but also a decrease in the acid strength of these sites [6]. Therefore, this is the main aim of this work, to evaluate the effect of the addition of small quantities of Li^+ and K^+, in their oxidized forms, to the CoMo catalysts supported on the hybrid Al_2O_3-MgO,

Table 1. Textural properties of the synthesized supports: specific area (S_{BET}), pore volume (V_P) and mean pore diameter (D_P).

	S_{BET} (m^2/g)	V_p (cc/g)	D_p (Å)
Al_2O_3	249	0.475	75
Al_2O_3-MgO	237	0.470	77
Al_2O_3-MgO-K_2O	258	0.465	78
K_2O/Al_2O_3-MgO	256	0.450	68
Al_2O_3-MgO-Li_2O	195	0.460	92
Li_2O/Al_2O_3-MgO	217	0.430	79

on the catalytic performance, in order to remarkably reduce the acidity of the catalysts; and to provide the catalysts with textural stability at ambient air exposure. On these catalysts, different functionalities were evaluated: HDS by using benzothiophene, HYD by using 1-octene and the HCK activity evaluated through the n-decane conversion. A preliminary study of the production of thiols under industrial hydrotreatment operating conditions was also performed by using the best catalyst.

2. Methods

2.1. Preparation of catalysts

The Al_2O_3-MgO support was prepared by the impregnation of γ-Al_2O_3 with an aqueous solution of $Mg(NO_3)$ 6 H_2O (Aldrich) in the required amount to reach 5 wt % of MgO, which is similar to the best composition previously reported by Klimova et al. [3]. As the alumina source, the pseudo-boehmite Catapal B^{TM} was used. The main support, the Al_2O_3-MgO, was impregnated with 1 wt % of the alkaline (Li_2O or K_2O) oxide precursor, (LiOH, Aldrich or KOH, Aldrich). Therefore, the last nominal composition of the mixture contained in the supports is 1 wt % of the alkaline oxide, 5 wt % of MgO and 94 wt % of Al_2O_3, approximately. The alkaline-modified supports were prepared by two single ways: a) The simultaneous mixture of $Mg(OH)_2$ plus the corresponding salt of Li or K; and alumina by using a binder of Catapal B according to the method described elsewhere [14], hereafter, these supports were called Al_2O_3-MgO-Li_2O or Al_2O_3-MgO-K_2O; b) once the Al_2O_3-MgO support was thermally treated by the drying (12 h, 100 °C) and calcination (4 h, 550 °C) steps; the addition of Li or K was performed by the impregnation of an aqueous solution containing the alkaline salt; henceforth this supports will be identified as Li_2O/Al_2O_3-MgO or K_2O/Al_2O_3-MgO. On these two series of supports, the impregnation of the precursors of the active phases, CoO and MoO_3, was simultaneously done by using the pore volume impregnation technique by means of an ammoniacal solution obtained according to a method described before [15], in order to avoid the dissolution of MgO during impregnation and the corresponding solid solution formation. The impregnation solutions were prepared by using $CoCO_3$, Aldrich analytical grade reagent; and MoO_3, JT Baker, analytical grade reagent.

2.2. Characterization of catalysts

The samples were characterized by N_2 physisorption measurements, Infrared (FT-IR) Spectroscopy, X-Ray powder diffraction, n-butyl amine titration and pyridine thermo- desorption. All the characterizations were performed on the aforementioned samples.

The N_2 physisorption was carried out to evaluate textural properties such as the specific surface area (S_{BET}), mean pore diameter (D_p) and total pore volume (Vt) of the aforesaid supports and catalysts. These measurements were done by using a Micromeritics ASAP 2010 system. The adsorption-desorption isotherms were collected, the S_{BET} was obtained by the multi-point Brunnauer-Emmet-Teller method (BET); and the mean pore diameter by the Barret-Joyner-Halenda method (BJH) from the desorption branch. Prior to the physisorption measurements, all the samples were outgassed at 270 °C for 3 h. In general, the errors found in repeated measurements of the surface area determinations were within 2-3.5 % of the total specific surface area.

Both the acid sites and fundamental structure were followed through the FT-IR spectra, which were collected by a Nicolet 510 spectrometer. The infrared spectroscopic monitoring of the adsorbed pyridine is an established tool to determine the acidity of solid acid catalysts. Advantages of this technique are: The Brönsted and Lewis acid sites can be distinguished because the IR spectra of adsorbed pyridine show characteristic differences; in situ thermal treatments can be performed on the catalysts and the strength distribution of the acid sites can be obtained by monitoring the pyridine thermodesorption. Taking into account that the Brönsted acid sites were analyzed through the 1515-1565 cm^{-1} region, where infrared bands are attributed to the pyridinium ion; and the bands assigned to the Lewis acid sites were studied through the 1435-1470 cm^{-1} region, the bands in this region are assigned to the pyridine coordinated bond, as it was reported by C. Emeis [16]. The samples were prepared in pressed disks and were cleaned and dehydrated by heating, under vacuum, at 250 ^oC for 1 h. The infrared spectra were recorded at room temperature, with 300 scans and a resolution of 4 cm^{-1}. Then, the pyridine chemisorption was carried out by recording the spectra at several temperature desorptions, which were: room temperature (25 ^oC approximately), 100 and 200 ^oC. The intensity of the Brönsted and Lewis bands helped to determine quantitatively the number of acid sites (Brönsted and Lewis); and their acid strength, which was expected to decrease. The obtained infrared spectra were processed and analyzed through the Omnic software. To corroborate that there is a decrease in the number of acid sites, the n-butylamine titration technique was also carried out, following the technique described by Gina Pecci et al [17]. To determine the crystalline phases, the X-Ray powder diffraction patterns were obtained in a Brucker Advance D-8 diffractometer in θ-θ configuration (Bragg Brentano) at room temperature by using CuKα radiation,

Table 2. Textural properties of the prepared catalysts: specific area (S_{BET}), pore volume (V_P) and mean pore diameter (D_P).

	S_{BET} (m^2/g)	V_p (cc/g)	D_p (Å)
$CoMo/Al_2O_3$	248	0.37	59
$CoMo/Al_2O_3$-MgO	192	0.36	72
$CoMo/Al_2O_3$-MgO-K_2O	200	0.33	78
$CoMo/K_2O/Al_2O_3$-MgO	150	0.30	77
$CoMo/Al_2O_3$-MgO-Li_2O	153	0.33	77
$CoMo/Li_2O/Al_2O_3$-MgO	168	0.34	76

and a graphite monocromator for the secondary beam. The measurements were carried out from 13° to 80° with a 2θ step of 0.02° with 2.2 in each point.

2.3. Catalytic Performance

In order to recreate industrial conditions, the simultaneous reactions of HDS of benzothiophene (BT) and HYD of 1-octene were chosen; the catalytic reactions were performed by using a flow micro-reactor in steady-state. The feed current was 2000 ppm of 1-octene (analytical grade reagent, J.T. Baker), 500 ppm of S as benzothiophene (analytical grade reagent, J.T. Baker) dissolved in n-decane (reactive grade, J.T. Baker); this feed composition was chosen to recreate real cuts. Before the catalytic evaluation, the catalysts were activated *in situ* at 300 °C (573 K) and atmospheric pressure in a CS_2/cyclohexane mixture in H_2 flow (40 ml/min). The reaction conditions were 380 °C (573K) and 19.4 atm (284 psia) with a H_2/HC ratio of 886 ft^3/bbl and a WHSV=12.5 h^{-1}. The catalytic activity of the following catalysts was evaluated: $CoMo/Al_2O_3$, $CoMo/Al_2O_3$-MgO, $CoMo/Al_2O_3$-MgO-Li_2O, $CoMo/Li_2O/Al_2O_3$-MgO, $CoMo/Al_2O_3$-MgO-K_2O, and $CoMo/K_2O/Al_2O_3$-MgO.
The products were quantified and identified by an Agilent 6890 gas chromatographer equipped with a capillary HP-1 column (50 m) with a flame ionization detector (FID); and complemented with an HP G1800B mass spectrometer with an electronic ionization detector. For the identification of the produced sulfur compounds (thiols), a Varian Chrompack 3800 CP chromatograph, equipped with a pulsed flame photometric detector (PFPD) was used.

3. Results and discussion

3.1. Characterization of supports and catalysts

Textural properties

The specific surface area (S_{BET}), total pore volume (V_p) and mean pore diameter (D_P) of the supports are shown in Table 1. In this table, it can be observed that the addition of magnesia causes a small drop in the surface area; and also the addition of Li_2O causes a decrease in the specific surface area with respect to the Al_2O_3-MgO support. The mean pore diameter showed a slight increase, whereas the total pore volume decreased; this indicates that the incorporation of magnesia blocked a small part of the pores in the alumina support. It is observed a different behavior for the K_2O modifier, where a slight increase in the specific surface area is obtained.

From the aforementioned results, it can be assumed that the addition of potassium oxide to the alumina-magnesia support promotes the recovery of part of the specific surface area as it can be observed in Table 1; however, the presence of K_2O has a negative effect on both the pore diameter (D_P) and pore volume (Vt), which could be probably due to the fact that K_2O is a non-porous material; and maybe, it promotes the blockage of pores. In this way, the highest reduction in the specific surface area is obtained in the catalysts prepared with Li_2O. Therefore, the MgO on alumina dissolution-redistribution process cannot be discarded. These results might suggest that the alkaline oxide does not help to increase the surface area; however, it could be helpful to preserve the surface area and give textural and structural stability to the MgO support avoiding the solid-solution formation.
The textural properties of the CoMo formulations are shown in Table 2. The addition of the Co and Mo phases causes a further decrease in the specific surface area in comparison to the corresponding support. The catalysts containing K present a slight decrease in the surface area, which is lower than that observed in the catalysts containing Li.

Structural properties

The crystallographic phases present in the supports and catalysts were determined by X-Ray powder diffraction (DRX). In Figure 1, the crystalline phases observed in the Al_2O_3-MgO-(K_2O) supports were mainly the γ-alumina and the periclase phases. The MgO (* periclase, JCPDS card: 4-0829) and the γ-Al_2O_3 crystalline phases (¤ alumina, JCPDS 10-425) were detected in both supports containing potassium; there is no evidence of diffraction lines due to K_2O (JCPDS 10-235), and this could be probably due to

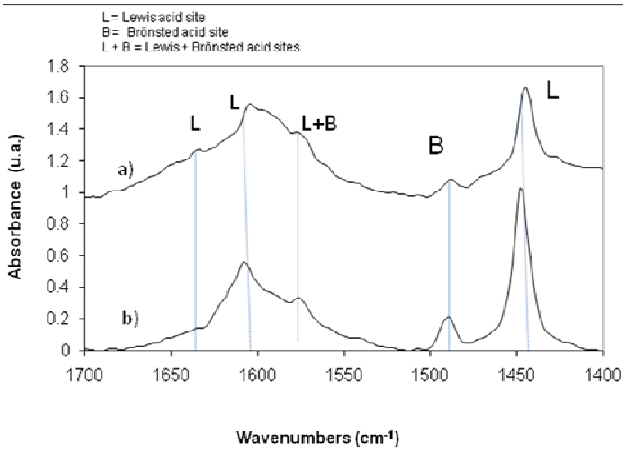

Table 4. Acid properties obtained by n-butylamine titration for the supports and their corresponding catalysts.

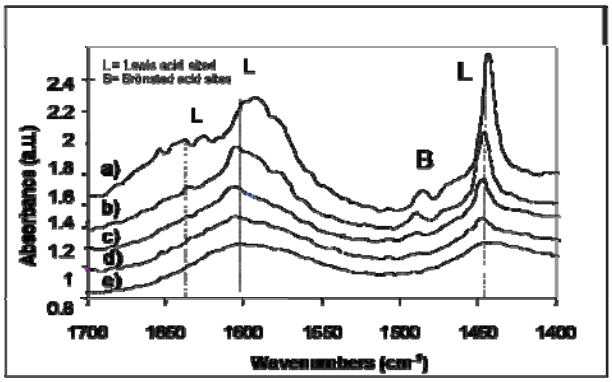

Figure 5. FT-IR Spectra of the pyridine thermodesorption of: the $CoMo/Al_2O_3$-MgO-K_2O formulation at different desorption temperatures: a) ambient temperature, b) 100 °C, c) 200 °C, d) 200 °C, e) 300 °C; and f) 400 °C.

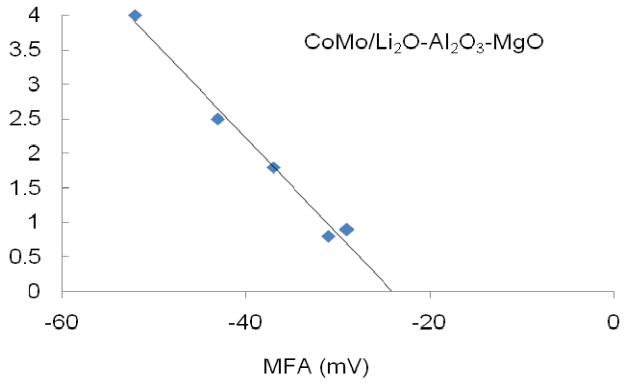

Figure 6. n-decane conversion versus maximum acid strength (MAS).

the fact that this oxide has an amorphous phase. However, the effect of the addition of an alkaline oxide gave some structural and textural stability to the Al_2O_3-MgO-K_2O support formulation, which could be related to the preservation of the surface area of the supports; and also to the catalyst formulations.

Figure 2 shows the diffraction profiles of the Al_2O_3-MgO supports doped with lithium oxide, some changes in the crystalline phases due to the addition of lithium can be observed. In these samples, the diffraction lines of an amorphous phase of γ-Al_2O_3 (JCPDS 10-425) are mainly observed; the diffraction lines of MgO are slightly evident; and there is no evidence of another crystalline oxidic phase attributed to the LiO_2 phase. The analogous X-diffraction patterns for the respective catalysts only showed a γ-alumina phase; there is no evidence of the CoO and MoO_3 crystalline phases; this could be probably due to a dilution effect and to the well dispersed Co-Mo phases, which probably are in crystallite sizes smaller than 40 Å. Additionally, the solid solution formation cannot be studied from these X-ray powder diffraction results because it is necessary to check the slight shift on the diffraction lines using an internal standard to take evidence about that fact.

Acid-base properties.

Figure 3 shows the infrared spectra of the catalytic supports and changes concerning the acid sites when MgO is added to the Al_2O_3 support. The alumina support mainly showed the characteristic bands of Lewis acid sites. According to the aforementioned, when magnesia is added to the alumina support, an intensity decrease in the infrared bands due to the pyridine interaction and lewis acid sites is evident; and also a decrease in the intensity of these bands was observed when the alkaline (potassium oxide) is added. The same effect was also observed when lithium oxide was added instead of potassium oxide, however these spectra are not shown on this work. These intensity reductions can be quantitatively related to the total number of Lewis acid sites (TNAS), which decrease in this case.

Figure 4 shows the pyridine thermodesorption spectra of the CoMo formulation doped with an alkaline and the respective $CoMo/Al_2O_3$ conventional formulation. In this figure, it is evident that there is a decrease in the total number of acid sites (TNAS) when the alkaline potassium oxide is added to the catalytic formulation, the number of acid sites were calculated by using the method described before by C. Emeis [16]. Something similar was observed for the formulation containing lithium, however the spectra are not shown in this work.

Figure 5 shows the thermodesorption spectra for the $CoMo/Al_2O_3$-MgO-K_2O formulation at several temperatures (T_{amb}, 100 °C, 200 °C and 300 °C). In this figure, it can be calculated the maximum acid strength (MAS) by comparing the intensity of the peak for Lewis acidity located at 1450 cm^{-1} at least at two different temperatures. The TNAS and MAS were calculated by the

Table 3. Acid properties obtained by pyridine thermodesorption for the different formulations.

Sample	**Lewis acidity** (mmol Py/g catalyst)	**Brönsted acidity** (mmol Py/g catalyst)	
	200 °C	200 °C	100 °C
Al_2O_3	0.017	0.00	0.00
Al_2O_3-MgO	0.015	0.00	0.00
Al_2O_3-MgO-K_2O	0.013	0.00	0.00
K_2O/Al_2O_3-MgO	0.010	0.00	0.00
Al_2O_3-MgO-Li_2O	0.013	0.00	0.00
Li_2O/Al_2O_3-MgO	0.012	0.00	0.00
CoMo/Al_2O_3	0.017	0.04	0.06
CoMo/Al_2O_3-MgO	0.015	0.04	0.02
CoMo/Al_2O_3-MgO-K_2O	0.010	0.01	0.01
CoMo/K_2O/Al_2O_3-MgO	0.009	0.01	0.01
CoMo/Al_2O_3-MgO-Li_2O	0.011	0.001	0.01
CoMo/Li_2O/Al_2O_3-MgO	0.011	0.001	0.01

Table 4. Acid properties obtained by n-butylamine titration for the supports and their corresponding catalysts.

Sample	**MAS** (mV)	**TNAS** (Meq/m^2)	
Al_2O_3	-222	0.0510	Al_2O_3
Al_2O_3-MgO	-145	0.0034	Al_2O_3-MgO
Al_2O_3-MgO-K_2O	-169	0.0021	Al_2O_3-MgO-K_2O
K_2O/Al_2O_3-MgO	-157	0.0018	K_2O/Al_2O_3-MgO
Al_2O_3-MgO-Li_2O	-97	0.0020	Al_2O_3-MgO-Li_2O
Li_2O/Al_2O_3-MgO	-191	0.0019	Li_2O/Al_2O_3-MgO
CoMo/Al_2O_3	-51	0.0410	CoMo/Al_2O_3
CoMo/Al_2O_3-MgO	-30	0.0032	CoMo/Al_2O_3-MgO
CoMo/Al_2O_3-MgO-K_2O	-30	0.0020	CoMo/Al_2O_3-MgO-K_2O
CoMo/K_2O/Al_2O_3-MgO	-37	0.0017	CoMo/K_2O/Al_2O_3-MgO
CoMo/Al_2O_3-MgO-Li_2O	-29	0.0019	CoMo/Al_2O_3-MgO-Li_2O
CoMo/Li_2O/Al_2O_3-MgO	-43	0.0018	CoMo/Li_2O/Al_2O_3-MgO

procedure previously reported by C. Emeis [16]. The results are shown in Table 3. Instead of the well-correlated results, the small values could have a high percent error; and besides the discrepancies about the accuracy of the technique, the TNAS and the MAS were also evaluated by other technique, such as the acid-base titration by using a strong base such as n-buthylamine (NBA) according to the technique reported before by Gina Pecci [17].

Changes in the total number of acid sites (TNAS) and acid site strength (maximum acid strength, MAS) were measured by using the acid-base titration; these results are shown in Table 4. The addition of MgO to alumina causes a decrease in the MAS and a sharp reduction in the TNAS as it was found by the pyridine chemisorption. The addition of K_2O to the Al_2O_3-MgO support gave an unexpected increase in the MAS; however, the addition of the alkaline metal causes a decrease in the TNAS, which is smaller than the one observed in the Al_2O_3-MgO support. A different behavior can be observed in the case of lithium incorporation; in this case, the lithium doped supports are more sensitive to the incorporation method, obtaining a

different behavior with respect to that in the MAS and TNAS.

For the CoMo catalyst, in Table 4, the data show that the precursor impregnation of the active phases produces a decrease in the MAS and TNSA in all the cases with respect to that observed in the corresponding supports. These phenomena are supposed to be caused by the hydroxyl group substitution by the corresponding oxidic phases of molybdenum and cobalt.

The comparison of the $CoMo/Al_2O_3$ and $CoMo/Al_2O_3$-MgO catalysts shows a sharp decrease in the MAS; and only a slight decrease in the TNAS.

3.2. Catalytic activity

The different formulations concerning the CoMo catalysts obtained in this work were evaluated; the results obtained for the catalytic performance are shown in Table 5. In this table, the conversion percent for the three model reactions are shown. The model reactions were: the hydrocracking of n-decane, hydrogenation of 1-octene; and also the hydrodesulfurization of benzothiophene. The conventional $CoMo/Al_2O_3$ catalytic formulation was used as the reference sample.

Hydrocracking activity.

The hydrocracking (HCK) reaction was evaluated with the conversion of the solvent (n-decane) by using the different catalyst formulations. The $CoMo/Al_2O_3$ reference catalyst presented by far the highest n-decane conversion, whereas the alkaline modified formulations did not show an important conversion percent as it is shown in Table 5. It can be corroborated that the decrease in the HCK reaction is related to the decrease in the acid sites of the catalysts when doped with an alkaline oxide. The HCK reaction presents low conversions (0.7-1.8 %), which present a decrease in the HCK conversion of 82 and 53.8 % with respect to the reference sample. In Figure 6, the MAS for the n-butyl amine titration versus the HYC conversion is depicted; this figure explores the influence of the maximum acid strength (MAS) of the catalysts on the n-decane conversion for the $CoMo/Li_2O$-Al_2O_3-MgO formulation; and it can be assumed that there is a direct relationship between the MAS and the HCK conversion; it can be concluded from this figure that the increase in the acid strength gives an increase in the n-decane conversion. Taking into account that the measurements were performed on the oxidic phases, a good correlation was observed.

Hydrodesulfurization activity

For all the samples, the catalytic activity in the HDS of BT was high, more than 95% in all the cases as it can be observed in Table 5. This is an expected result since BT is not considered as one of the most refractory sulfur compounds. The activity of catalysts for the HDS of BT presents a +/- 2 % deviation from the conversion obtained with the conventional formulation, which indicates that the alkaline addition does not exert a great influence on the HDS function, which is maintained.

Hydrogenation activity

As it was mentioned, the hydrogenation of olefins reduces the octane number, which is expected in a minor proportion when catalysts doped with an alkaline oxide are used; a moderate hydrogenation activity is also expected. This function was followed with the hydrogenation of 1-octene, which was chosen because of its easy hydrogenation. The total conversion results are presented in Table 5. It is necessary to mention that in this conversion, other reactions like the hydrocracking are present. In order to observe the hydrogenation, it could be more appropriate to analyze the n-octane yield.

The highest hydrogenation activity was obtained with the $CoMo/Al_2O_3$ catalysts, a decrease in the hydrogenation function was not only observed with the MgO addition to the conventional formulation but also when the alkaline oxide was added, which is in good agreement with the literature; and with the results previously reported by Klimova et al. [3], where it was mentioned that the addition of MgO causes a decrease in the HYD activity. The addition of the alkaline compound (Li or K) causes a

Table 5. Catalytic evaluation results and overall conversions for benzothiophene and n-decane; and conversion and 1-octene yield.

Catalysts	**[1]Conversion** (%)			**[2] Octane yield**
	octene	benzothiophene	decane	
$CoMo/Al_2O_3$	100	96.9	3.9	97.0
$CoMo/Al_2O_3$-MgO	98.6	98.2	0.6	90.7
$CoMo/Al_2O_3$-MgO-K_2O	98.7	97.3	0.7	85.7
$CoMo/K_2O/Al_2O_3$-MgO	93.0	95.1	1.8	83.7
$CoMo/Al_2O_3$-MgO-Li_2O	99.3	98.5	0.7	92.0
$CoMo/Li_2O/Al_2O_3$-MgO	97.1	96.7	0.9	83.7

[1] The 1-octene conversion was directly calculated from the area percentages determined by chromatographic methods, using the following equation: 1-octene conversion = $[(1\text{-octene}_0 - 1\text{-octene})/(1\text{-octene}_0)]x100$. The conversions for benzothiophene and n-decane were similarly calculated.

[2] n-octane yield $=[(\text{octane})/(1\text{-octene}_0 - 1\text{-octene})]x100$.

further decrease in this property. The catalyst with the smallest n-octane yield is the $CoMo/Al_2O_3$-MgO-K_2O; but due to the small n-octane yield plus the small hydrocracking activity, the $CoMo/LiO_2$-Al_2O_3-MgO catalyst is considered as the best option.

4. Conclusions.

The addition of an alkaline (K or Li) oxide to the hybrid Al_2O_3-MgO support promotes textural stability; textural properties remain after alkaline incorporation, it seems that alkaline an metal addition using a non-aqueous solution promotes that specific surface area does not change a lot. It can also be concluded that the alkaline addition causes a decrease in the total number of acid sites (TNAS) in both the support and the corresponding CoMo catalysts. This decrease in the TNAS could be related with the decrease in the HCK activity and also with the decrease in the HYD activity, whereas the HDS function is maintained. So, it can be concluded that the high catalytic performance in the selective HDS is related to the alkaline modified catalysts, where a good option could be the $CoMo/LiO_2$-Al_2O_3-MgO formulation.

Acknowledgements

The financial support given by the IMP (Instituto Mexicano del Petróleo) through the FIES 98-116-II program is amply acknowledged. The authors want to thank Dra. Ma. Elena Llanos for her help in the N_2 physisorption measurements; and Engineer René Zarate Ramos for his valuable comments. D. Solis thanks CONACyT for the support given through the "Programa de Retención/Consolidación Institucional"; and the SIEA-UAEM for the support given through the 2349, 2368/UAEM and SEP-PROMEP 103.5/07/2572 Projects.

References

[1] A. Humphries, T. Reid, Ch. Kushler; Hydrocarb. Process, 51 (2003).
[2] H. Shimada, T. Sato, Y. Yoshimura, J. Hiraishi, A. Nishijima, J. Catal**. 110**, 275 (1988)
[3] M. Zdrazil, T. Klicpera; Appl. Catal. A-Gen. **216,** 41 (2001)
[4] T. Klimova, D. S. Casados, J. Ramirez, Catal. Today, **43,** 135 (1998).
[5] T. Cortez y G. Hernández. Efecto de la adición de Potasio y Lantana a catalizador convencional $CoMoAl_2O_3$. Revista del IMIQ, **42**, 43 (2002).
[6] B. Caloch, M. S. Rana and J. Ancheyta; Catalysis Today **98,** 91 (2004).
[7] J. Cinibulk, P. J. Kooyman, Z. Vit, M. Zdrazil, Catal. Lett. **89**, 147 (2003).
[8] D. Solis, T. Klimova, J. Ramírez, T. Cortez; Catal. Today **98**, 99 (2004).
[9] M. Zdrazil, Catal. Today **86**, 151 (2003).
[10] J. Cinibulk, P. J. Kooyman, Z. Vit, M. Zdrazil, Catal. Lett. **89**, 169 (2003).
[11] R. West, Basic Chemical solid state; Wiley pp. 56 (1993)
[12] J. Cinibulk, P.J. Kooyman, Z. Vit, M. Zdrazil, Catal. Lett. **89**, 147 (2003).
[13] P.A. Chernavskii, G. V. Pankina, V. V. Lunin, Catal. Lett. **66**, 121 (2005).
[14] Gervasini, A.; Fenyvesi, J.; Auroux, A. Langmuir **12**, 5356 (1996).
[15] R. J. Bertolacini, T. Sue-A-Quan, US Pat 4140626, (1977).
[16] C. Emeis; Journal of catalysis **47**, 18 (1985)
[17] R. Cid, G. Pecci, Appl. Catal., **14**, 15 (1985).